Reliability Engineering and System Safety 279 (2027) 113812



Contents lists available at ScienceDirect

Reliability Engineering and System Safety

journal homepage: www.elsevier.com/locate/ress



Beyond the V-shaped recovery curve: An automatic identification system-based two-phase framework for port resilience under tropical cyclones

Ruikai Sun [a], Huanhuan Li [b], Zaili Yang [a,*]

[a] Liverpool Logistics, Offshore and Marine (LOOM) Research Institute, Liverpool John Moores University, Liverpool, UK
[b] School of Engineering, University of Southampton, Southampton, UK

ARTICLE INFO

Keywords:
Port resilience
Tropical cyclones
AIS data
Post-cyclone congestion
Functional recovery
Two-phase framework

ABSTRACT

Extreme weather events, particularly tropical cyclones, pose substantial challenges to maritime transport and global supply chains. This study develops an AIS-based two-phase resilience framework to quantify port operational responses to tropical cyclone impacts using 76 port-cyclone cases in East Asia. The framework distinguishes direct disruption from post-cyclone congestion and introduces a Port Service Performance (PSP) indicator and seven resilience indices to quantify the magnitude, duration and cumulative impact of both phases. Under the identification settings, 56 of the 76 cases exhibit identifiable direct disruption followed by post-cyclone congestion. Within the proposed framework, this sequence can be represented as a conditional W-shaped pattern in PSP. Linear mixed-effects modelling shows that the identified congestion phase is associated with significantly longer vessel waiting times, while berthing time does not increase significantly, indicating that post-cyclone service deterioration is primarily reflected in vessel queuing. Regression results show that a higher container share is associated with shorter direct and overall recovery durations, while facility capacity and port-city GDP per capita are associated with smaller maximum deviations during congestion. More frequent cyclone exposure is also associated with lower cumulative disruption impacts. The proposed framework extends conventional single-phase resilience assessment by capturing congestion-related functional loss following the initial recovery of vessel activity and provides empirical insights for post-cyclone port recovery and congestion management.

1. Introduction

Extreme weather events, particularly tropical cyclones, pose substantial challenges to maritime transport networks and global supply chains. As critical nodes in global supply chains, ports are responsible for handling over 80% of the world's cargo by volume [1]. Consequently, the capacity of ports to sustain continuous and stable operations is fundamental to maintaining global economic growth [2]. Unlike rare natural disasters such as earthquakes or tsunamis, tropical cyclones constitute a recurrent and high-frequency hazard that port authorities must manage on a regular basis. Forming over extensive tropical and subtropical oceans, tropical cyclones occur most frequently in the Northwest Pacific, where the annual average reaches approximately 26 events [3]. By contrast, the North Indian Ocean experiences the fewest occurrences, averaging approximately 7% of the global mean number per year [4].

The impacts of tropical cyclones on port operations are complex. The most immediate result of these impacts is operational disruptions. To ensure operational safety, ports typically suspend ship movements, cargo handling, and yard operations prior to cyclone landfall [5]. These measures often result in ships queuing at anchorages or rerouting to alternative ports and finally cause widespread schedule delays. Economic losses follow rapidly. The interruption of port operations directly reduces revenues for ports, shipping companies, and cargo owners [6,7], while physical damage to port assets such as cranes and warehouses leads to high maintenance costs [8]. In addition, port closures disrupt hinterland transport and the global maritime network. These disruptions will lead to cargo congestion, extended delivery times, and broader logistics inefficiencies [9]. Therefore, accurately assessing and enhancing port resilience has become a crucial challenge in maritime logistics

* Corresponding author.
E-mail address: Z.Yang@ljmu.ac.uk (Z. Yang).

https://doi.org/10.1016/j.ress.2026.113812
Received 19 March 2026; Received in revised form 2 November 2026; Accepted 5 November 2026
Available online 7 November 2026
0951-8320/© 2026 The Author(s). Published by Elsevier Ltd. This is an open access article under the CC BY license (http://creativecommons.org/licenses/by/4.0/).

research.

Existing studies on port resilience, particularly those focusing on single-system operational performance, have mainly relied on the existing traditional recovery curve frameworks in the literature [5,10]. These models generally assume that port operations gradually recover after a disruption until the port call number returns to or exceeds the pre-event baseline [11]. However, this assumption oversimplifies the post-disruption dynamics observed in real-world operations. Our large-scale empirical analysis reveals that, although ship numbers at most ports return to baseline levels after a tropical cyclone, their service performance often fails to recover accordingly due to frequently occurring post-cyclone congestion. This congestion can generate a second period of operational loss after the direct cyclone impact, which conventional single-phase resilience curves are unable to represent. This observation reveals a fundamental measurement problem in the operational resilience of ports. The return of vessel activity does not mean that the port has restored its normal service function. When delayed vessels return within a short period, vessel numbers may recover or even exceed the baseline while waiting times continue to rise. A resilience assessment based solely on vessel activity may therefore identify recovery before service conditions are restored. In this study, post-cyclone congestion is examined as evidence of this divergence between activity recovery and functional recovery.

To address this research gap, this paper proposes a two-phase framework for measuring port operational resilience under tropical cyclones based on large-scale Automatic Identification System (AIS) ship data. The main contribution of the framework is that it empirically decouples the full impact of tropical cyclones into two distinct phases, "direct disruption" and "post-cyclone congestion". The framework also introduces the Port Service Performance (PSP) indicator as an AIS-derived proxy for the ship-activity dimension of port operational status. PSP quantifies the magnitude of deviation from the pre-cyclone vessel-activity baseline, while relative vessel activity presents the direction of this deviation. Within this framework, a W-shaped PSP pattern provides a conditional representation of the sequence of normal operation, direct disruption, initial activity recovery, post-cyclone congestion and final activity recovery. These indicators simultaneously quantify port dynamics during both phases, thereby overcoming the limitations of traditional resilience models.

The main contributions of this study are as follows:

(1) Development of a new port performance metric and resilience framework.

An AIS-derived PSP indicator is introduced to measure the magnitude of deviations in vessel activity from normal operating conditions. Combined with the direction of relative vessel activity, the indicator distinguishes direct cyclone disruption from post-cyclone congestion. Seven resilience indices are then developed to quantify the magnitude, duration and cumulative impact of the two phases. This framework extends conventional single-phase resilience assessment by formally representing congestion-related functional loss after the initial recovery of vessel activity. The W-shaped pattern is used as a conditional diagnostic representation within this framework.

(2) Empirical identification of ports' response patterns to cyclone shocks.

Using 76 port-cyclone cases across 12 tropical cyclone events in East Asia, the study identifies heterogeneous operational responses. Under the reference settings, 56 cases exhibit identifiable direct disruption followed by accepted post-cyclone congestion. LME modelling further shows that the identified congestion phase is associated with longer vessel waiting times, supporting its operational relevance.

(3) Analysis of resilience determinants through the proposed indices.

The seven resilience indices are used to examine associations between port characteristics, including facility capacity, port type and recorded cyclone exposure frequency, and resilience outcomes across both phases. The findings provide actionable insights for port authorities and shipping companies to improve preparedness and operational strategies.

The remainder of this paper is organised as follows. Section 2 systematically reviews the literature on tropical cyclone impacts and port resilience. Section 3 details the methodology, including the development of the two-phase resilience framework, the conditional W-shaped PSP representation and the framework validation. Section 4 presents the datasets, validation results, and driver analysis. Section 5 discusses the key findings and managerial implications. Section 6 concludes the paper and outlines future research directions.

2. Literature review

This section reviews the literature relevant to measuring port operational resilience under tropical cyclone impacts. It is organised around three connected themes. Section 2.1 reviews empirical evidence on cyclone-related port disruption and recovery, with particular attention to AIS-based changes in vessel activity, delays and post-reopening accumulation. Section 2.2 examines performance-based approaches to port resilience assessment and considers whether the recovery of activity-based indicators adequately represents the restoration of normal service conditions. Section 2.3 draws on the recovery-process perspective and queueing theory to explain why vessel activity may recover before service performance, resulting in post-cyclone congestion. Together, these three strands establish the theoretical and empirical basis for distinguishing direct disruption from post-cyclone congestion and activity recovery from functional recovery.

2.1. Tropical cyclone disruption and recovery at ports

Tropical cyclones can greatly disrupt port operations through temporary closures and restrictions on ship movements. These impacts reduce or delay port call numbers and may generate wider effects on shipping schedules and connected logistics systems. Existing studies have examined these impacts from different perspectives. For example, some studies quantified the economic consequences of cyclone-related port disruptions [6,12], while Wang et al. [13] further examined the associated risks and adaptation measures. These studies demonstrate that even short-term interruptions can generate great impacts for ports and their users.

The increasing availability of AIS datasets has enabled more direct observation of how maritime traffic responds to tropical cyclones. Verschuur et al. [5] used empirical shipping data to examine port disruptions caused by natural hazards and identified relationships between disruption duration and hazard intensity. Huang et al. [14] compared maritime network conditions before, during and after Tropical Cyclone Ma-on and found clear changes in connectivity, stability and transport efficiency, with different recovery speeds across the affected network. At the vessel level, Zhang et al. [9] combined AIS data with Bayesian networks to examine tropical cyclone-related transport delays and identify the effects of cyclone, ship and port characteristics. Other studies have examined how cyclone exposure affects maritime network reliability and connectivity by modelling the disruption or removal of ports affected by cyclones [15,16]. Together, these studies show that tropical cyclone impacts can be observed not only through physical damage or economic losses, but also through changes in vessel activity, delays and network performance.

Despite these advances, empirical research has mainly focused on the immediate disruption caused by tropical cyclones or on changes in shipping network conditions around the event. Comparatively less attention has been paid to how port operations evolve after the direct cyclone impact has ended. In particular, the recovery of vessel activity

does not necessarily imply that the disruption has been fully resolved. Empirical evidence from Hurricane Matthew shows that vessel activity can surge after port reopening, while accumulated vessels may take additional time to process and experience increased dwell times [17]. Similar post-disruption increases in port activity have been observed as ports temporarily increase throughput to recapture disrupted cargo flows [5]. However, these post-cyclone dynamics have rarely been incorporated into port resilience assessment as a distinct phase of operational loss. A further gap is that many empirical studies are based on individual events, specific ports or limited geographical areas, which makes it difficult to determine whether observed disruption and recovery patterns are common across different port-cyclone cases. Large-scale, high-frequency operational data therefore provide an opportunity to examine port responses throughout the disruption and recovery process and to distinguish different forms of post-cyclone operational change. This provides the empirical basis for a more detailed examination of how port resilience and recovery should be measured.

2.2. Performance-based assessment of port resilience

The concept of resilience varies across disciplines, although its core principle remains consistent: it refers to a system's ability to withstand external shocks or disturbances and recover to a stable state [18,19]. In the context of port operations, resilience can be defined as the port's capacity to continue providing services to ships and cargoes when external events cause operational disruptions [5,20–22]. Existing port resilience studies have examined this capacity from system, organisational and network perspectives. Organisational studies mainly focus on management capability and decision-making using approaches such as expert assessment and Bayesian networks [23–25], while network studies examine connectivity, interdependence and the propagation of disruption among ports [26–28]. The present study focuses on system resilience, particularly the temporal evolution of port operational performance during disruption and recovery.

A common approach to system resilience assessment is to represent system performance as a function of time before, during and after a disruption. Resilience curves provide a quantitative description of performance loss and subsequent recovery, from which the magnitude, duration and cumulative impact of a disruption can be measured [18,19]. This performance-based approach has also been applied to port systems. For example, Verschuur et al. [5] used empirical vessel activity to identify the onset, duration and recovery of port disruptions caused by natural disasters. Gu et al. [29] examined port resilience through congestion-related operational indicators, while Gu et al. [30] assessed resilience across absorb, adapt and recover stages using a network data envelopment analysis approach. These studies demonstrate the value of operational data for moving resilience assessment beyond static infrastructure characteristics or expert judgement.

However, the interpretation of a resilience curve depends strongly on how system performance is defined. Port performance can be represented through different dimensions, including vessel activity, cargo throughput, waiting time, berth utilisation and other measures of service efficiency. These indicators describe related but different aspects of port operations and do not necessarily recover simultaneously. In particular, the return of vessel activity to its pre-disruption level indicates that ship calls have resumed, but it does not, by itself, demonstrate that the port has restored normal service conditions. A port may accommodate a normal or above-normal number of vessels while experiencing longer queues and delays. Existing performance-based resilience methods rarely focus on situations in which different dimensions of port performance recover at different times. This creates a need to distinguish the recovery of vessel activity from the recovery of service function when assessing port operations after a disruption.

2.3. Theoretical mechanism of activity and functional recovery

Recovery is a dynamic process through which system performance is progressively restored after a disruption rather than a single point at which an activity indicator returns to its reference level. The trajectory and rate of performance restoration are therefore important dimensions of system resilience [31]. In port operations, this perspective is particularly relevant because the resumption of vessel movements does not necessarily indicate that normal service conditions have been restored.

Queueing theory provides a theoretical basis for explaining this divergence. A queueing system is characterised by an arrival process and finite service capacity, with waiting occurring when demand cannot be served immediately. Little's Law further establishes the relationship between the average number of entities in a system, their arrival rate and their average time in the system [32]. This principle has been widely applied in port operations, where vessels represent arriving service demand and berths and associated handling resources provide service capacity. Previous studies have used queueing approaches to examine the relationship between vessel arrivals, berth capacity, berth utilisation and vessel waiting time [33–36]. During a tropical cyclone, port closures or operational restrictions temporarily reduce effective service capacity and defer scheduled vessel calls. Once operations resume, delayed vessels may return within a compressed period. If this temporary demand exceeds available handling capacity, queues and waiting times increase until the backlog is absorbed. Similar mechanisms have been used to explain disruption-induced congestion in maritime transport systems [37]. The present study therefore draws on queueing theory to explain this transient demand-capacity imbalance.

This mechanism distinguishes three stages of recovery. Reopening refers to the resumption of service availability, activity recovery to the return of vessel activity towards its pre-disruption level, and functional recovery to the restoration of normal service conditions. These stages need not occur simultaneously. Vessel activity may recover while congestion and waiting times remain elevated, and service performance may therefore deteriorate again before final recovery. From this perspective, post-disruption congestion represents a capacity-constrained stage of the recovery process rather than an independent external disruption.

On this theoretical basis, a W-shaped PSP pattern may emerge when several conditions occur sequentially. First, the disruption must cause an identifiable temporary reduction in vessel activity. Second, a substantial proportion of affected vessel calls must be delayed, allowing deferred demand to return after operations resume. Third, these delayed vessels must return within a sufficiently concentrated period, and the resulting temporary demand must exceed the port's effective service capacity, generating vessel accumulation and congestion-related service loss. The complete trajectory may not emerge when the initial disruption is limited or disrupted calls are cancelled. These mechanisms motivate the distinction between direct disruption and post-cyclone congestion. Their representation as a W-shaped pattern is conditional on the PSP definition and the observed sequence of vessel-activity deviations.

2.4. Research gaps

Although existing studies have advanced understanding of tropical cyclone impacts and port resilience, several critical gaps remain that shape the contributions of this study. First, existing operational resilience measures do not fully capture port status across the complete disruption and recovery cycle. Most research focuses on the immediate disruption or the subsequent return of port activity, without explicitly distinguishing activity recovery from the restoration of normal service conditions or quantifying potential performance loss during post-cyclone congestion. Second, the empirical understanding of how ports respond dynamically to cyclone shocks remains limited. Previous studies often focus on single-port case studies or individual events, providing limited evidence of common disruption and recovery patterns across

different ports and cyclone events. Third, few resilience assessments combine high-frequency port activity data with ship-level service outcomes to examine whether identified recovery states correspond to actual changes in operational performance. This limits the empirical validation of activity-based resilience measures. Finally, current research provides only limited insight into the driving factors of resilience across the entire disruption period. There are few quantitative comparisons of how port characteristics, including capacity, infrastructure, operational scale and prior cyclone experience, affect resilience during both the direct disruption and post-cyclone congestion phases.

These gaps motivate the development of an AIS-based two-phase resilience framework and the Port Service Performance indicator, the large-scale empirical analysis of 76 port-cyclone cases, the validation of the identified operational states using LME modelling, and the introduction of seven resilience indices to examine the drivers of resilience across both phases. Within this framework, a W-shaped PSP pattern serves as a conditional representation of the sequence in which direct disruption is followed by post-cyclone congestion.

3. Methodology

This section introduces the methodological framework developed to quantify port resilience in the context of tropical cyclone impacts. Building on large-scale AIS observations and cyclone event records, the methodology develops an AIS-based two-phase framework for measuring port operational resilience. The framework identifies and quantifies direct disruption and post-cyclone congestion, evaluates whether the identified operational states correspond to changes in ship service conditions, and examines the factors associated with resilience in both phases. Accordingly, Section 3.1 outlines the overall framework. Section 3.2 introduces the AIS-based two-phase resilience framework

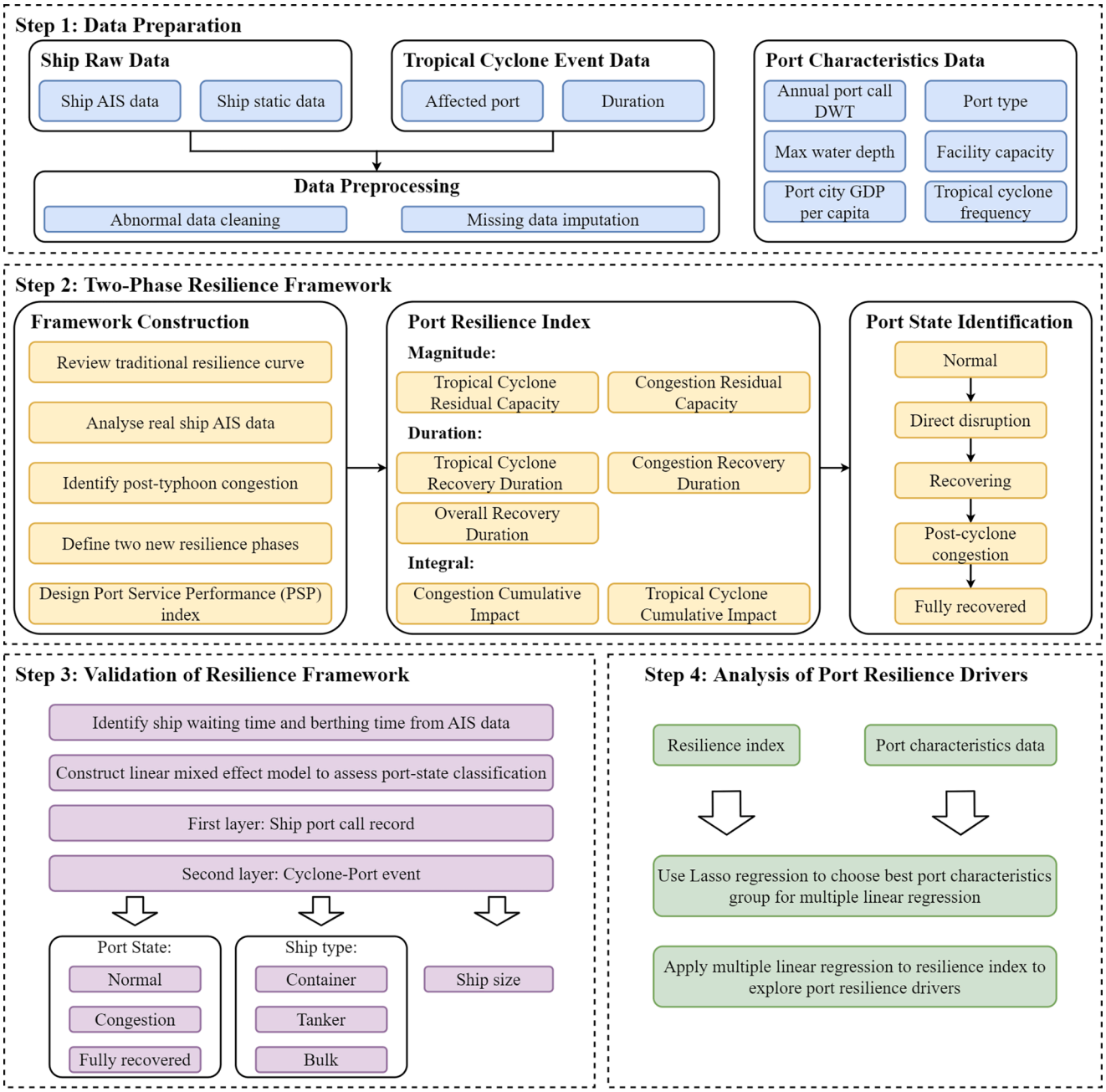


Fig. 1. The overall framework of this study.

and the PSP indicator. Section 3.3 describes new resilience indices. Section 3.4 presents the analytical procedures for identifying the phases of tropical cyclone impacts. Section 3.5 shows the validation strategy using ship activity data. Together, these interactive components provide a coherent and data-driven foundation for assessing how ports recover from disruptions caused by tropical cyclones.

3.1. The proposed framework

The overall research framework of this study is illustrated in Fig. 1. This is an AIS data-driven empirical framework for analysing port resilience under tropical cyclone impacts. The framework consists of four main components: data preparation, two-phase resilience measurement, criterion validation, and resilience driver analysis. In the first step, three categories of data are collected, including ship AIS data, tropical cyclone event data, and port characteristic data. To ensure the quality and consistency of the case analyses, outliers are removed from the dataset, and missing values are imputed using statistical procedures.

The second step constructs the AIS-based two-phase resilience measurement framework. Based on AIS data from 76 port-cyclone cases, the analysis reveals that many ports experience a sharp increase in the number of ships after the cyclone, forming a distinct post-cyclone congestion phase. This phenomenon can generate a second period of operational loss that conventional single-phase recovery models do not explicitly represent. To address this limitation, the total tropical cyclone impact is decomposed into two sequential phases, direct disruption and post-cyclone congestion. An AIS-derived PSP indicator is then introduced to quantify the magnitude of vessel-activity deviation from the pre-cyclone baseline. Relative vessel activity is used together with PSP to preserve the direction of the deviation and distinguish reduced vessel activity from excessive vessel accumulation. PSP is therefore used as a proxy for the ship-activity dimension of port operational status rather than as a comprehensive measure of port service performance. Based on these indicators, the framework distinguishes direct disruption from post-cyclone congestion and quantifies the magnitude, duration and cumulative impact of both phases. When both phases occur sequentially, the resulting vessel-activity deviations can be represented as a conditional W-shaped PSP pattern within the framework.

The third step focuses on validating the two-phase resilience framework using ship activity data. An LME model is applied to examine whether classifying port states based on PSP accurately reflects operational efficiency. The dependent variables include ships' waiting time and berthing time, both derived from AIS activity records. In contrast, port state is defined by three categories: normal, post-cyclone congestion, and fully recovered. Ship type and ship size are included as covariates to control for heterogeneity in ship characteristics. Two hypotheses are tested: first, that ships have significantly longer waiting times during the port-cyclone congestion phase than during the normal phase; and second, that waiting times in the fully recovered phase do not differ significantly from those in the normal phase. These results are used to evaluate the validity of the proposed two-phase resilience framework.

The final step explores the drivers of port resilience, thereby providing an empirical foundation for port disaster management strategies. Seven new resilience indices are calculated from the two-phase resilience framework, together with six categories of port-specific characteristics. Lasso regression is first employed to select the most relevant explanatory variables for each resilience index, followed by multiple linear regression analysis to evaluate the direction and significance of their effects. This approach enables an in-depth understanding of how port characteristics impact resilience during the disruption and congestion phases, offering practical insights to improve port adaptability under extreme weather conditions.

3.2. Two-phase resilience framework under tropical cyclone impact

To investigate how port operational resilience evolves under tropical cyclone impacts, this study develops an AIS-based two-phase resilience framework. Fig. 2 illustrates process of the framework construction. Fig. 2(a) shows the state-of-the-art resilience curve model in existing literature to describe port or waterway recovery after a tropical cyclone [5,10,38]. The x-axis represents time, and the y-axis represents system performance, which in empirical port studies can be measured by the number of ships calling at the port within a given period, denoted as P (T). The red shaded area indicates the duration of the tropical cyclone's formation and dissipation. T_0 and T_f mark the overall time window of the case study, while T_h, T_e, T_d, and T_s correspond to the stages of the tropical cyclone. They represent tropical cyclone formation, the initial impact on the target port, the end of the direct impact, and the start of recovery, respectively. Because tropical cyclone impacts are usually short-lived, the interval between T_d and T_s is often brief and can sometimes be treated as a single point. T_f represents the point when the port reaches its expected performance level, which may be higher or lower than the pre-tropical cyclone baseline.

However, analysis of real AIS data reveals that only a small number of ports return directly to their pre-tropical cyclone conditions. In most cases, ports experience a phase of post-cyclone congestion before back to normal. Fig. 2(b) illustrates this pattern using the case of tropical cyclone Kong-rey, which struck the Port of Ningbo-Zhoushan in November 2024. The x-axis shows time in four-hour intervals (with time 0 representing T_d), while the y-axis indicates the number of ships in port. The black line shows the 4-hourly ship count, and the blue line represents the one-day moving average. The blue shaded area highlights a period when ship arrivals far exceeded the normal pre-tropical cyclone level. This phenomenon highlights the inadequacy of the traditional framework, as it fails to distinguish between recovery and congestion. In operational terms, this surge does not necessarily reflect improved performance or resilience, while it signals delayed arrivals that reduce service quality [29]. Under the conventional resilience framework, however, such conditions would be misinterpreted as a full recovery once ship counts return to their previous level. This limitation underscores the need for a new resilience model capable of recognising and quantifying post-disruption congestion.

To address this limitation, Fig. 2(c) illustrates the proposed two-phase resilience framework, which explicitly incorporates post-cyclone congestion into the assessment of port recovery following direct disruption. Within this framework, the W-shaped pattern is a conditional representation in PSP rather than an independently established empirical recovery curve. Its appearance depends on both the definition of PSP and the sequence of vessel-activity deviations. The framework therefore focuses on distinguishing and measuring the two operational phases, while ship-level service outcomes are examined separately to assess the operational meaning of the identified states. The horizontal axis represents time, while the vertical axis represents the AIS-derived PSP indicator. As shown in Eq. (1), PSP(t) is calculated based on the ship count at time t (N_t) and the average ship count during a pre-tropical cyclone baseline period (N_{base}), defined as the 28 days preceding the tropical cyclone in this paper. This duration aligns with previous studies [5,14,10] and balances representativeness with data stability, avoiding the potential influence of other unrelated events that might arise in longer reference windows. This indicator captures both port disruptions and congestion as deviations from normal conditions. This indicator also conducts standardisation for cross-port comparisons. Relative vessel activity is defined as A_t, which retains the direction of the deviation from normal activity. Values below 1 indicate reduced vessel activity, whereas values above 1 indicate vessel accumulation. Because PSP captures the magnitude but not the direction of the deviation, it is interpreted jointly with A_t. In the new model, additional time points are introduced: T_{e2} marks when the port first returns to normal operations

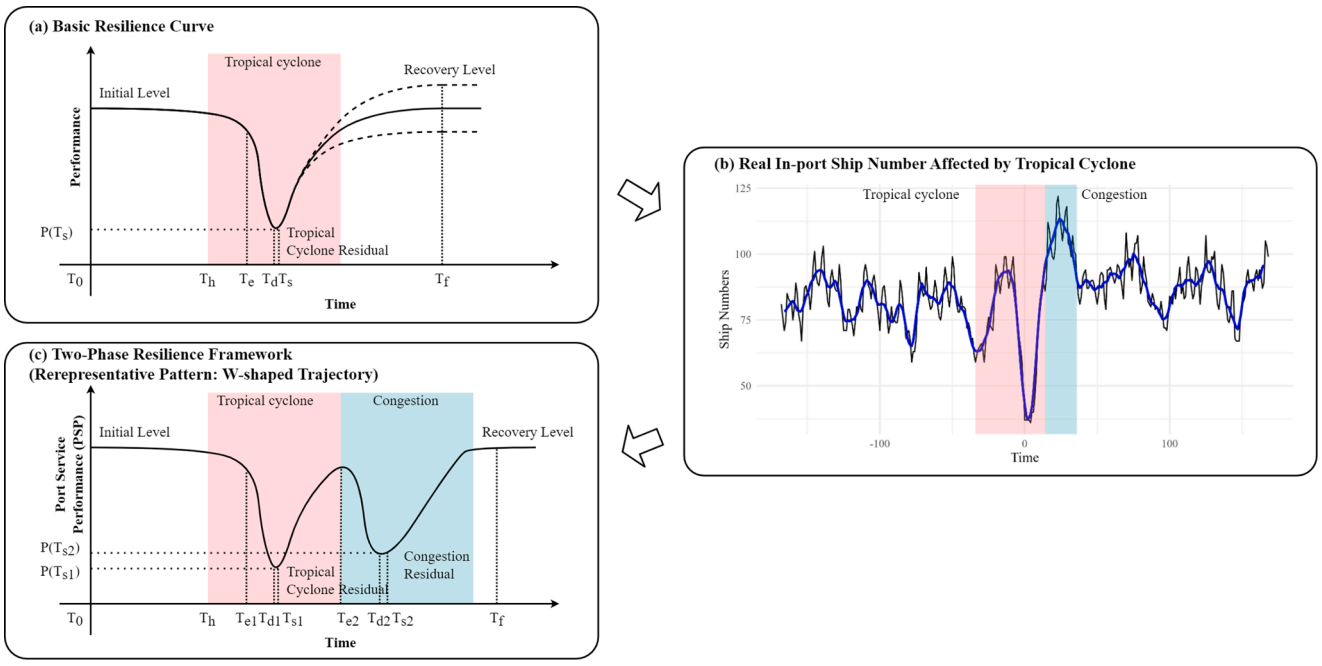


Fig. 2. From basic resilience curve to two-phase resilience framework (a: Basic Resilience Curve; B: Real In-port Ship Number Affected by Tropical Cyclone; C: Two-Phase Resilience Framework.).

and when congestion begins; T_{d2} and T_{s2} denote the end and the easing of the congestion phase, respectively. Together, these stages describe a more realistic recovery pathway and enable a more holistic assessment of port resilience to tropical cyclone disruptions.

$$\mathrm{PSP(t)} = 1 - \frac{|N_t - N_{base}|}{N_{base}},\ A_t = \frac{N_t}{N_{base}} \tag{1}$$

3.3. Port resilience index

To evaluate the resilience performance of different ports under tropical cyclone impacts, this study adopts three categories of resilience metrics: magnitude, duration, and integral [19]. The magnitude category includes two indicators: Tropical cyclone Residual Capacity (TRC) and Congestion Residual Capacity (CRC). As shown in Eqs. (2) and (3), these indicators represent the lowest level of port functionality maintained during the tropical cyclone impact and post-tropical cyclone congestion phases, respectively.

$$\mathrm{TRC} = \mathrm{PSP}(T_{d1}) \tag{2}$$

$$\mathrm{CRC} = \mathrm{PSP}(T_{d2}) \tag{3}$$

The duration category comprises three indicators: Tropical cyclone Recovery Duration (TRD), Congestion Recovery Duration (CRD), and Overall Recovery Duration (RD). As defined in Eqs. (4)–(6), these indices capture the time required for the port to recover from a tropical cyclone shock, to recover from the congestion, and to fully return to its expected performance level from the tropical cyclone shock.

$$\mathrm{TRD} = T_{e2} - T_{s1} \tag{4}$$

$$\mathrm{CRD} = T_f - T_{s2} \tag{5}$$

$$\mathrm{RD} = T_f - T_{s1} \tag{6}$$

Finally, the integral category quantifies the cumulative impact of each disruption phase. Two measures are defined: Tropical cyclone Cumulative Impact (TCI) and Congestion Cumulative Impact (CCI). As shown in Eqs. (7) and (8), these indicators integrate the deviation of PSP(t) from its normal level $\mathrm{PSP_{base}(t)}$ over time, representing the total loss of functionality during each stage. Since PSP is standardised, here $\mathrm{PSP_{base}(t)}$ equals 1.

$$\mathrm{TCI} = \int_{T_{e1}}^{T_{e2}} (\mathrm{PSP_{base}(t)} - \mathrm{PSP(t)}) \tag{7}$$

$$\mathrm{CCI} = \int_{T_{e2}}^{T_f} (\mathrm{PSP_{base}(t)} - \mathrm{PSP(t)}) \tag{8}$$

These three categories of indices holistically describe the depth, duration, and extent of port functional deviation and recovery following tropical cyclone disruptions.

3.4. Port state identification

Identifying the operational state of a port based on the PSP indicator is a key step in constructing the resilience model. First, the normal operational level of each port is determined using the average PSP value over a pre-tropical cyclone reference period [39]. The 28 days preceding each tropical cyclone event are selected as the baseline period. Given that the original PSP series with a 4-hour interval exhibited substantial short-term fluctuations, a six-period (24-hour) moving average is applied in this study. This procedure aims to filter out high-frequency noise and thereby capture the actual trend of PSP accurately. The smoothed series is denoted as $\mathrm{PSP_{smooth}}$. A port is in an abnormal state when its $\mathrm{PSP_{smooth}}$ value falls below 0.8, meaning that the number of ships in port is <80% or greater than 120% of the normal level. When fluctuations remain within ±20%, they are considered part of normal operational variation, driven by market cycles or routine scheduling [5,40]. Because tropical cyclone impacts on ports often last less than a day [41], and the data are recorded at four-hour intervals, the port is considered finally recovered when its $\mathrm{PSP_{smooth}}$ values remain within the normal range for at least 48 consecutive hours (12 data points). This rule prevents temporary fluctuations from being misclassified as recovery or new disruption. Since the direct effects of tropical cyclones on port operations typically last only 1–2 days and follow a concentrated disruption-recovery pattern [9,14], congestion appearing more than a

week after the first-phase recovery is unlikely to be directly caused by the cyclone. Thus, such cases are excluded to ensure causal consistency. These instances are therefore regarded as unrelated to the tropical cyclone event.

Fig. 3 illustrates this identification process using the case of Tropical Cyclone Lingling that struck the Port of Pyeongtaek in September 2019. The x-axis represents time in four-hour intervals, and the y-axis shows the PSP value, with the blue line indicating the normal condition threshold. The light blue line is PSP_{smooth}. From the figure, it shows that after time 0 (the end of direct impact), the port's performance recovered to normal by the eleventh time point. Congestion began around the fifteenth time point, followed by a temporary recovery near the twenty-ninth time point before a new deviation until the thirty-seventh point. Finally, the port returned to normal on the forty-sixth point. This example demonstrates the robustness of the proposed state identification method. A sensitivity analysis was conducted to examine the dependence of the response classification on the identification settings. The normal operating band was varied to ±15% and ±25%; the moving average window to 12, 16, 20, 28, 32 and 36 h; the final stable-recovery requirement to 12, 24 and 36 h; and the congestion association window to 5, 6, 7 and 8 days. Each parameter was varied individually while the remaining parameters were held at their reference values. The same 76 cases, observation series and classification hierarchy were retained. Sensitivity was assessed using the counts of the four response types with the reference classification. The results are reported in Appendix A, Table A.1.

3.5. Linear mixed effect model

To verify whether the PSP can effectively represent the system performance along the resilience curve, a Linear Mixed-Effects Model (LME), also known as a Linear Multilevel Model, is employed. Specifically, a two-level random-intercept and random-slope model is estimated to test whether there are significant differences in ship waiting times across port states defined by the PSP indicator. Following the definitions established in Section 3.4, the normal phase refers to the waiting times of ships arriving within the 28 days prior to the formation of a tropical cyclone; the post-cyclone congestion phase corresponds to the port congestion period identified from the PSP curve; and the fully recovered phase represents the waiting times of ships arriving after congestion has ended but still within the analysis window.

The multilevel modelling framework partitions the data into two hierarchical levels: the first level represents individual observations, and the second level represents groups [42]. In this study, Level 1 corresponds to ship-level port call records, while Level 2 corresponds to port-cyclone cases, that is, observations of individual ports under specific tropical cyclone events. Within the same port-cyclone case, ship call records share common environmental and baseline conditions, thus exhibiting a nested data structure. Two LME models are estimated separately, using ship waiting time and berthing time as the dependent variables. The fixed effects include both explanatory variables and covariates. The key explanatory variable is port state (Normal, Post-cyclone congestion, and Fully recovered), and the covariates are ship type (Container, Bulk, and Tanker) and ship size, as both have been shown to influence waiting time [43,44]. Port state and ship type are categorical variables, with Normal and Container set as the reference categories and converted into dummy variables for regression estimation. To better capture heterogeneity in phase-specific responses, the model also includes a random slope for the port-state variable, allowing the rate of change across phases to vary among different port-cyclone cases. The specific model is expressed in Eq. (9), where Y_{ij} denotes the waiting time of port-call record i in port-cyclone case j. $D_{cong.ij}$ and $D_{reco.ij}$ are dummy variables representing the port state, while $D_{bulk.ij}$ and $D_{tank.ij}$ are dummy variables representing ship type. β_{0j} is the intercept term, and β_{1j}-β_{5j} are the regression slopes, with ε_{ij} denoting the residual error term. γ represents the overall mean intercept, μ_{0j} is the random intercept, and $\mu_{1j}$and μ_{2j} are the random slopes, capturing case-specific deviations from the overall relationship.

$$
\begin{aligned}
&\textit{Level } 1: \\
&Y_{ij} = \beta_{0j} + \beta_{1j}D_{cong.ij} + \beta_{2j}D_{reco.ij} + \beta_{3j}D_{bulk.ij} + \beta_{4j}D_{tank.ij} + \beta_{5j}DWT_{ij} + \varepsilon_{ij} \\
&\textit{Level } 2: \\
&\beta_{0j} = \gamma_{00} + \mu_{0j}; \\
&\beta_{1j} = \gamma_{10} + \mu_{1j}; \\
&\beta_{2j} = \gamma_{20} + \mu_{2j}
\end{aligned}
\tag{9}
$$

If the coefficient of $D_{cong.ij}$ is statistically significant, it indicates that ship waiting times during the congestion phase are significantly longer than those in the normal phase, suggesting that the port indeed experienced actual congestion following the tropical cyclone. Conversely, if the coefficient of $D_{reco.ij}$ is not significant, it implies that ship waiting times during the fully recovered phase do not differ substantially from those in the normal phase, thereby confirming the reliability of the PSP indicator proposed in this study.

4. Experimental results and analysis

4.1. Experimental datasets and preprocessing

To evaluate and validate the proposed two-phase resilience framework, this study compiled a dataset covering twelve tropical cyclone events that affected the East Asian region between 2019 and 2024. These events are identified using natural disaster records from IMF PortWatch [45], combined with ship AIS data and ship technical information from LSEG [46]. From these events, 122 port-cyclone cases are identified. Using AIS-derived daily ship arrival data, 46 cases are excluded because their annual ship calls are too limited to determine whether variations in ship numbers resulted from cyclone disruptions or normal commercial fluctuations. The spatial distribution of the remaining cases is shown in

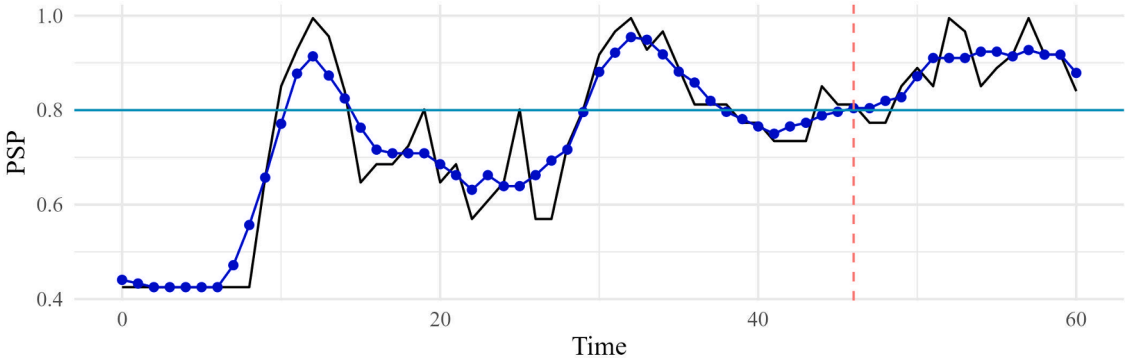


Fig. 3. Example of port state identification.

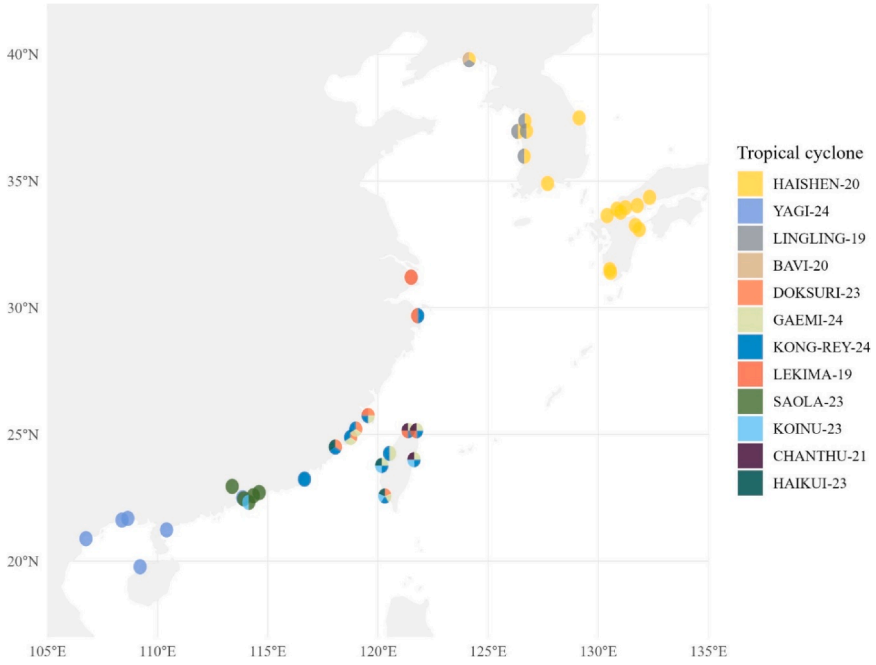


Fig. 4. Study area and tropical port-cyclone cases.

Fig. 4. Kaohsiung experienced the highest number of cyclone impacts, with five occurrences, while Fuzhou, Hualien, Keelung, Mailiao, and Taipei were each affected four times. Other ports in the dataset experienced no more than three tropical cyclone events during the study period.

Following previous research, the temporal scope of each tropical port-cyclone case in this study is defined as the four weeks before and after the duration of the cyclone, consistent with established approaches [5,14]. The analysis focuses on three major ship types: tankers, bulk carriers, and container ships. Passenger ships are excluded because of their different operational characteristics [47]. Only ships larger than 5000 DWT are included, as smaller ships often have incomplete AIS records, and this threshold aligns with the IMO standards. For each port, the spatial scope of data collection is defined as an 80-nautical-mile radius. The Fourth IMO Greenhouse Gas Study evaluated port-database catchment radii of 20, 40 and 80 nautical miles and reported that a 40-nautical-mile radius matched approximately 95% of the ports in the two validation datasets [48]. Given that the present study also seeks to retain offshore waiting and vessel movements that may extend beyond the port during cyclone-related restrictions, the upper 80-nautical-mile radius examined in the IMO study was adopted as a more conservative initial data-extraction window. Port calls are identified from vessel anchorage, berthing and departure behaviour, thereby limiting the inclusion of unrelated transit traffic. A port call is measured from a ship's entry into this zone, through its cargo-handling operations, until its departure from the berth area. For ships travelling between two ports located within the same 80-nautical-mile radius, the period begins when the ship leaves the previous port's berth area, completes its cargo operations, and departs again. These consistent definitions ensure the comparability of port cases across different locations.

After screening and integration, a total of 20,398 ships with corresponding AIS and technical data are collected. As the datasets contained outliers and missing values, several preprocessing procedures are applied. For the AIS data, positional anomalies are detected and removed by cross-validating ship coordinates with real-time speed information, while missing values are interpolated using the average of the preceding and following time points. For missing values in the technical dataset, the stepwise multiple nonlinear regression method proposed by Sun et al. [49] is employed to perform imputation and ensure data completeness.

4.2. Port resilience analysis

Using the methodology described in Section 3, this study calculated the port resilience indices for 76 port-tropical cyclone cases. Based on the results, the effects of tropical cyclones on port operations can be grouped into four representative response types, each reflecting a distinct pattern of disruption, recovery, and post-event dynamics. Fig. 5 illustrates these four patterns according to the variation in PSP and the number of ships in port relative to the pre-cyclone baseline. Fig. 5(a) shows the changes in PSP, while Fig. 5(b) presents the corresponding fluctuations in ship numbers. The red dashed line indicates the end of the cyclone impact period, and the grey shaded area represents the normal operating range, defined in Section 3.4 as the baseline ±20%. Fig. 5(c) displays the distribution of the four response types across all cases.

As shown in Fig. 5(a), Type I (Tropical Cyclone Kong-Rey, Ningbo-Zhoushan) represents a disruption-with-congestion pattern, in which vessel activity declines during the cyclone, initially returns towards the normal range, and subsequently rises above the baseline because of post-cyclone vessel accumulation. As deviations on both sides of the baseline reduce PSP, this sequence produces two distinct periods of operational deviation in the PSP trajectory. Within the two-phase framework, this response type is represented by a conditional W-shaped PSP pattern. Type II (Tropical Cyclone Yagi, Chiwan) illustrates a disruption-without-congestion pattern, where vessel activity falls during the cyclone but returns to the normal range without a subsequent congestion phase. Type III (Tropical Cyclone Saola, Hong Kong) represents congestion without an identifiable direct disruption, where vessel activity shows limited initial reduction but subsequently exceeds the normal range. Type IV (Tropical Cyclone Lingling, Incheon) represents an impact with a sustained new-equilibrium pattern, where vessel activity remains persistently outside the pre-cyclone normal range. In these cases, a distinct post-cyclone congestion phase cannot be reliably identified. Fig. 5(b) gives a clearer picture of the port operation trend.

The distribution of these four types, shown in Fig. 5(c), demonstrates the heterogeneity of port responses to tropical cyclone impacts and the ability of the proposed two-phase framework to accommodate different

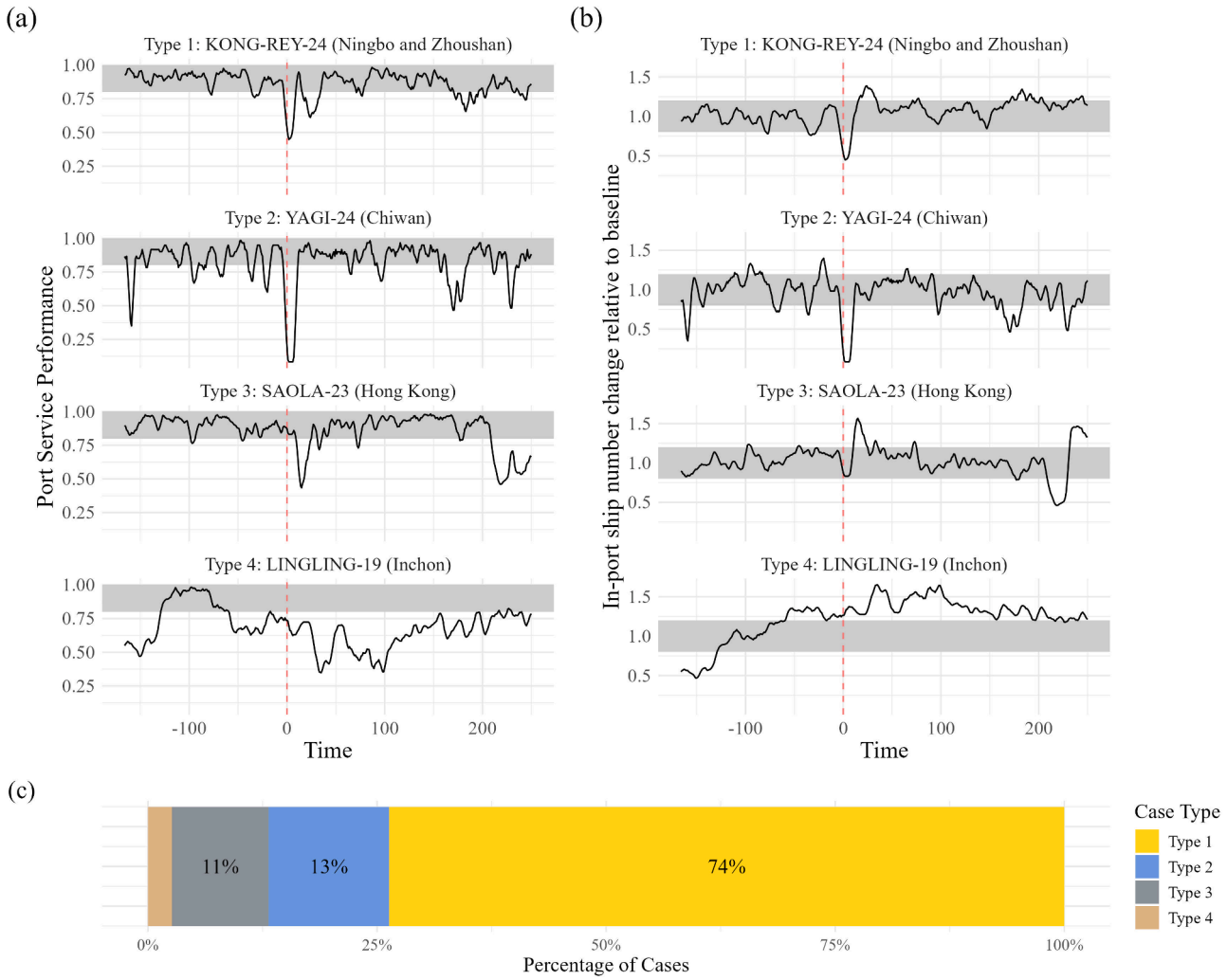


Fig. 5. Classification of port resilience patterns under tropical cyclone impacts.

disruption and recovery trajectories. Among the 76 port-cyclone cases, 56 cases (73.7%) exhibit both direct disruption and subsequent post-cyclone congestion, 10 cases (13.2%) exhibit direct disruption without subsequent congestion, 8 cases (10.5%) exhibit congestion without an identifiable direct disruption, and 2 cases (2.6%) move towards a different operational equilibrium. These 56 cases establish the prevalence of the disruption-with-congestion response under the reference identification settings. The remaining cases demonstrate the conditional nature and boundary conditions of the complete trajectory. The sensitivity analysis indicates that the predominance of the disruption-with-congestion response is maintained under the tested individual parameter changes (Appendix A, Table A.1). The Type I count ranged from 52 to 56 cases, corresponding to 68.4%–73.7% of the sample, compared with 56 cases under the reference specification. Type I remained the largest and majority response class in every tested specification. These results support the stability of the predominant response type.

Table 1 reports descriptive statistics for the 56 Type 1 cases. All seven indicators are calculated and summarised for this same subset, providing a consistent basis for comparing the direct-disruption and post-cyclone congestion phases. The other 20 cases remain part of the classification analysis but are not pooled into these descriptive summaries. Indices requiring a recovery endpoint were recorded as NA when that endpoint was not identified within the observation period. The descriptive statistics of the resilience indicators reveal a clear contrast between the direct disruption and post-cyclone congestion phases. The mean TRC was 0.36, indicating that the minimum PSP during the direct disruption phase averaged 0.36. During the post-cyclone congestion phase, the CRC averaged 0.13 but showed substantial variability (SD = 0.49), with several ports even recording negative values. As defined in Eq. (1), a greater deviation of the PSP from 1 indicates a stronger impact on service performance. When the number of ships in port exceeds twice the benchmark level, the CRC value becomes negative, reflecting a situation of excessive congestion. This finding confirms that post-cyclone congestion frequently leads to secondary operational inefficiency. Both the CRD and the CCI averaged 147 h and 77.8, respectively, which are considerably higher than those observed during the direct cyclone phase. These descriptive results indicate that the post-cyclone congestion phase was longer and associated with a greater cumulative PSP deviation than the direct disruption phase. The mean overall recovery

Table 1
Descriptive summary of port resilience indices for Type 1 port-cyclone cases.

Port resilience index	Mean	SD	Min	Max	Median	N
TRC	0.359	0.189	0.000	0.777	0.384	56
CRC	0.135	0.492	−1.871	0.725	0.252	56
TRD	59.143	26.922	4.000	108.000	58.000	56
CRD	147.286	143.897	12.000	612.000	94.000	56
RD	292.071	168.141	100.000	780.000	244.000	56
TCI	46.945	27.630	6.240	116.633	38.987	56
CCI	77.825	82.438	3.302	397.032	42.016	56

duration was 292 h, showing that port operational recovery can extend substantially beyond the period of direct cyclone disruption.

4.3. Validation of the two-phase resilience framework

Based on the port-state identification results described in Section 4.2, this study employed two LME models with random intercepts and random slopes to examine how post-cyclone congestion influences ship berthing and waiting times. This analysis also serves to verify the applicability of the proposed two-phase resilience framework and the PSP-based state classification. The two LME analyses use 59,902 port-call records from 11,295 unique vessels across 56 port-cyclone cases. The same vessel may contribute more than one record through repeated calls or inclusion in different cases.

For ship waiting time (Table 2), all fixed-effect variables, except for the Fully Recovered phase, are statistically significant. The intercept corresponds to the reference category, average size container ships during the normal phase, with an average waiting time of 0.66 days. The estimated coefficients indicate the differences in waiting time across phases and ship types. During the congestion phase, waiting times are significantly longer than those in the normal phase, increasing on average by 0.15 days. By contrast, the Fully Recovered phase shows no significant difference from the normal phase. These results support the validity of the proposed two-phase resilience framework by showing that the identified congestion phase corresponds to a measurable deterioration in ship service conditions, while waiting times return to their normal level after congestion has dissipated.

Differences among ship types are also significant. Compared with container ships, bulk carriers and tankers experience longer waiting times by 0.49 days and 0.47 days, respectively. Ship size has a positive relationship with waiting time: each additional 1000 DWT increases waiting time by approximately 0.001 days. Regarding random effects, the baseline variation in average waiting time across ports is about ±0.33 days (around eight hours), while the standard deviation of port-specific responses during the congestion phase reaches ±0.17 days (around four hours). This suggests substantial variation in congestion effects among ports, with some experiencing much greater delays than others.

For ship berthing time (Table 3), the results show that both ship type and tonnage have significant effects on berthing duration. The intercept corresponds to the reference category, average size container ships during the normal phase, with an average berthing time of 0.55 days. Berthing time during the post-cyclone congestion phase does not differ significantly from that during the normal phase ($\beta = 0.038$ days, $p = 0.082$). By contrast, the fully recovered phase is associated with a small but statistically significant reduction in berthing time ($\beta = -0.039$ days, $p = 0.011$), equivalent to approximately one hour. On average, bulk carriers and tankers remain at berth 1.02 days and 0.60 days longer, respectively, than container ships. Ship size also exerts a positive influence on berthing time, with every additional 1000 DWT associated with an increase of approximately 0.003 days. The random effects reveal that baseline variations in berthing time across ports are around ±0.37 days, while inter-port differences during the congestion phase reach about ±0.09 days, suggesting moderate heterogeneity in operational efficiency among ports.

Table 2
Results of ship waiting time from the LME model.

Fixed effects:					
Variables	Estimate	Std. Error	df	t value	p-value
γ_{00}	0.662	0.045	53.6	14.700	<0.001 ***
$D_{cong.ij}$	0.155	0.032	40.1	4.910	<0.001 ***
$D_{reco.ij}$	−0.008	0.021	45.6	−0.377	0.708
$D_{bulk.ij}$	0.494	0.010	59,100	49.100	<0.001 ***
$D_{tank.ij}$	0.472	0.013	58,700	37.200	<0.001 ***
DWT_{ij}	0.001	<0.001	59,700	13.000	<0.001 ***
Random effects:					
Groups	Variables	Variance		Std. Dev.	
Case id	μ_{0j}	0.107		0.327	
	$D_{cong.ij}$	0.029		0.171	
	$D_{reco.ij}$	0.018		0.134	
Residual	ε_{ij}	0.848		0.921	

Table 3
Results of ship berth time from the LME model.

Fixed effects:					
Variables	Estimate	Std. Error	df	t-value	p-value
γ_{00}	0.553	0.050	51	11.000	<0.001 ***
$D_{cong.ij}$	0.038	0.021	35	1.790	0.082
$D_{reco.ij}$	−0.039	0.014	21	−2.810	0.011 *
$D_{bulk.ij}$	1.020	0.009	59,500	109.000	<0.001 ***
$D_{tank.ij}$	0.598	0.012	59,200	50.900	<0.001 ***
DWT_{ij}	0.003	<0.001	59,800	46.700	<0.001 ***
Random effects:					
Groups	Name	Variance		Std. Dev.	
Case id	μ_{0j}	0.136		0.369	
	$D_{cong.ij}$	0.007		0.087	
	$D_{reco.ij}$	0.005		0.073	
Residual	ε_{ij}	0.724		0.851	

4.4. Analysis of port resilience drivers

This section examines how port characteristics influence the seven resilience indices using Lasso and multiple linear regression analyses. This analysis examines associations between the measured port characteristics and resilience indices. The observational design does not identify causal effects or directly test the mechanisms underlying these associations. In general, a port's physical infrastructure, including its size and functional type, affects its resilience to tropical cyclone impacts, while regional socioeconomic conditions, such as population and economic level, shape its recovery capacity. The analysis also examines whether recorded cyclone exposure frequency is associated with the resilience indices.

Seven explanatory variables are selected to represent these factors: annual port call DWT, port type (share of container and bulk calls), maximum water depth, facility capacity, port-city GDP per capita, and tropical cyclone frequency. Annual port call DWT is calculated as the total deadweight tonnage of all ships calling at the port in the year when the cyclone occurred. Port type is expressed as the proportions of container and bulk carriers, with the tanker share excluded to avoid multicollinearity, since the three proportions together equal one. Maximum water depth is derived from the greatest ship draught recorded among the ships visiting that year. Facility capacity is measured by the total number of terminals and anchorages. Port-city GDP per capita is obtained from national or commercial statistical databases, and tropical cyclone frequency is measured as the number of cyclone events that affected each port during 2019–2024.

Because the model included seven explanatory variables, Lasso regression is first applied to identify the most relevant predictors before conducting multiple linear regression. The Lasso model is tuned using 10-fold cross-validation, and the optimal penalty parameter (λ) is selected at the point where the cross-validated mean squared error reaches its minimum. When a regression coefficient reduces to zero, the Lasso model interprets the corresponding variable as unimportant or unstable for predicting that resilience index and excludes it from the final specification. All variables are standardised before estimation.

The coefficient estimates are summarised in Table 4. Significant predictors are identified for TRC, CRC, TRD, RD, and TCI. In contrast, the bulk percentage and maximum water depth are not selected by any model, since the bulk percentage can be inferred from the container share, and maximum water depth appears to have limited influence on the resilience indices. No candidate predictors were retained by LASSO

Table 4
Regression coefficients of the LASSO models.

Term	TRC	CRC	TRD	CRD	RD	TCI	CCI
(Intercept)	0.222	−0.703	5.219	4.542	5.609	3.831	3.852
Bulk percentage	/	/	/	/	/	/	/
Container percent	−0.042	/	−0.515	/	−0.166	/	/
GDP per capita	/	0.007	−0.057	/	/	/	/
Facility capacity	0.024	0.174	/	/	/	/	/
Annual port call DWT	/	0.017	−0.019	/	/	/	/
Max water depth	/	/	/	/	/	/	/
Tropical cyclone frequency	0.015	/	−0.063	/	/	−0.059	/
Lambda coefficient	0.013	0.132	0.038	0.081	0.090	0.105	0.224

Note: "/" indicates that the coefficient was shrunk exactly to zero and the predictor was not selected by LASSO.

for CRD or CCI at the selected penalty. This result concerns variable selection within the present sample and specification; such factors remain potential explanatory variables for future research.

After identifying the relevant explanatory variables for each resilience index through LASSO regression, this study conducts multiple linear regression analyses to examine whether the selected variables have significant effects on the resilience indices. Because LASSO selects no explanatory variables for CRD and CCI, no post-LASSO multiple linear regression with explanatory variables is estimated for these two outcomes. Table 5 therefore reports results only for TRC, CRC, TRD, RD, and TCI, for which at least one explanatory variable is selected. All variables, except for the container and bulk percentages, are logarithmically transformed to approximate the normality of residuals and reduce the influence of scale differences.

For TRC, the coefficient of facility capacity is positive, with a p-value of 0.053, indicating a marginally significant effect. For CRC, both facility capacity and GDP per capita show significant positive effects, suggesting that ports with greater facility capacity can maintain higher residual capacity during both the direct disruption and post-cyclone congestion phases. Ports located in economically developed regions also tend to sustain higher service levels under extreme weather conditions. For TRD and RD, the container percentage shows a significant negative relationship with both indices, indicating that ports with a higher share of container ships recover more quickly from tropical cyclone disruptions and achieve faster overall recovery. This may result from the high degree of standardisation and shorter turnaround times in container operations, which facilitate a quicker resumption of normal activities after disruptions. For TCI, tropical cyclone frequency shows a significant negative effect, suggesting that ports more frequently exposed to tropical cyclones experience lower cumulative losses.

5. Discussion and implications

This study provides a new perspective on understanding port resilience under tropical cyclone impacts. It addresses the limitations of conventional assessment frameworks and offers managerial insights for port authorities and policymakers.

5.1. Redefining port recovery

The main insight of this research is that cyclone-related operational loss does not necessarily end with the direct disruption but may continue through post-cyclone congestion. The empirical results show that 64 of the 76 analysed port-cyclone cases (84.2%) experience post-cyclone congestion, either following an identifiable direct disruption or without a clear initial disruption. Among the 56 Type 1 cases, the mean congestion recovery duration (CRD = 147 h) and cumulative impact (CCI = 77.8) are also greater than those observed during the direct disruption phase (TRD = 59 h; TCI = 46.9). These findings challenge recovery assessments that identify the return of vessel activity to or above its pre-event baseline as the completion of port recovery.

The empirical response types also help interpret the conditions under which a W-shaped PSP pattern may emerge. Such a pattern requires an identifiable reduction in vessel activity during the cyclone, an initial return towards the baseline, and subsequent vessel accumulation. This sequence may arise when affected vessel calls are delayed, when these vessels return within a concentrated period after reopening, and when the resulting demand exceeds the port's effective service capacity. Conversely, this pattern may not emerge when the initial disruption is limited, disrupted calls are cancelled or successfully rerouted, arrivals resume gradually, or sufficient spare capacity absorbs the returning demand. Cases moving towards a different post-event operating level further indicate that recovery does not necessarily return to the original baseline. These conditions reinforce that the W-shaped trajectory should be interpreted as a conditional archetype of the broader two-phase framework.

The LME results clarify the operational meaning of the identified congestion phase. Vessel waiting times are significantly longer during this phase than during normal operations, showing that the activity-based classification corresponds to observable differences in service conditions. This supports distinguishing vessel-activity recovery from the restoration of normal service conditions. It does not, however, establish that service performance temporarily recovered between the direct-disruption and congestion phases. The W-shaped PSP pattern therefore remains a conditional diagnostic representation, while the empirical evidence concerns the operational states and their associated service outcomes.

By explicitly representing post-cyclone congestion within the

Table 5
Results of the multiple linear models.

Resilience index	TRC		CRC		TRD		RD		TCI	
Variables	Estimate	P-value	Estimate	P-value	Estimate	P-value	Estimate	P-value	Estimate	P-value
(Intercept)	0.185	0.001	−3.737	0.015	6.085	0.000	5.715	0.000	4.031	0.000
Container percent	−0.099	0.100	/	/	−0.566	**0.039**	−0.447	**0.034**	/	/
GDP per capita	/	/	0.153	**0.017**	−0.090	0.249	/	/	/	/
Facility capacity	0.042	**0.053**	0.244	**0.037**	/	/	/	/	/	/
Annual port call DWT	/	/	0.101	0.243	−0.047	0.506	/	/	/	/
Tropical cyclone frequency	0.023	0.107	/	/	−0.083	0.151	/	/	−0.137	**0.037**

recovery process, the proposed two-phase resilience framework extends conventional single-phase assessments that may not capture service deterioration following the initial recovery of vessel activity. The framework distinguishes direct disruption from post-cyclone congestion and quantifies the magnitude, duration and cumulative impact associated with each phase through separate resilience indices. TRC, TRD and TCI characterise the magnitude, duration and cumulative deviation associated with the direct disruption phase, whereas CRC, CRD and CCI characterise the corresponding dimensions of the post-cyclone congestion phase.

This distinction is important because a port may show strong resistance to immediate shocks (low TCI) but weak congestion management capacity (high CCI), resulting in lower overall resilience. The proposed framework therefore provides a more detailed diagnostic basis for evaluating cyclone-related port operational resilience across both phases. This will help port operators to better develop their resilience plans from an overall perspective and the shipping companies to evaluate the resilience of their ports of call to minimise any negative effects generated by the poor post-cyclone congestion management capacity.

5.2. Emergency management during tropical cyclone impacts

The results highlight the importance of treating cyclone preparedness as a continuing operational responsibility. Recorded cyclone exposure frequency is negatively associated with cumulative direct-disruption impact, indicating that recovery outcomes differ across ports operating under different exposure conditions. This finding provides a useful basis for comparing preparedness arrangements and disruption-management practises across frequently and less frequently affected ports. For port authorities, preparedness should therefore extend beyond event-specific emergency mobilisation to include regularly reviewed operating procedures, drills and coordination arrangements. Knowledge sharing among ports can support this process by making established response practises available beyond the locations where they were developed.

The analysis further shows that ports with a higher proportion of container ships recover more quickly, both in terms of TRD and RD. This outcome may be related to the greater level of standardisation, automation, and scheduling efficiency that characterises container handling operations. Container terminals typically employ advanced digital systems for berth allocation, cargo tracking, and yard management, which enable faster clearance and more predictable turnaround times once disruptions subside. In contrast, bulk and tanker ports often display longer turnaround times because their handling processes rely on specialised equipment, strict safety procedures, and coordination with shore-based facilities such as storage tanks and conveyors [50]. These complexities extend the time needed to restore normal throughput after disruption. Therefore, efforts to strengthen resilience in bulk and tanker ports should prioritise process standardisation, the adoption of digital scheduling tools, and improved coordination among terminal operators, shipping lines, and hinterland logistics providers. In this context, best practises learnt from ports of the best performance can be used to improve the process of realising the prioritisation. By streamlining operations and enhancing real-time visibility, these measures can reduce recovery delays and build adaptive capacity to cope with future extreme weather events.

5.3. Post-cyclone congestion management strategies

The findings suggest that port contingency planning should address not only the immediate disruption caused by tropical cyclones but also the congestion that may develop as vessel activity returns. The LME analysis identifies a significant association between the congestion state and longer vessel waiting times, whereas no statistically significant association with berthing time is detected. This distinction is consistent with congestion being reflected primarily in delays before berthing rather than in the duration of berth occupancy. From a resilience perspective, restoring vessel activity to its normal range should therefore be distinguished from clearing the accumulated demand and returning port operations to a stable state.

The results also indicate the importance of distinguishing congestion severity from congestion duration. Facility capacity is positively associated with CRC, corresponding to smaller peak congestion-related deviations under the definition of this index. This association suggests that facility provision is relevant to the severity of the observed congestion response, although it does not establish a causal effect of capacity. In operational terms, limiting the maximum accumulation of vessels and reducing the time required to clear congestion are separate objectives. Capacity planning can consider the ability to accommodate concentrated vessel demand, while recovery planning should address the processing of accumulated traffic following the resumption of operations. These objectives can be assessed using separate measures of peak congestion and clearance duration.

Port-city GDP per capita is also positively associated with CRC after accounting for facility capacity in the selected model. This finding indicates that differences in congestion severity are associated with both measured port characteristics and the surrounding economic context. GDP per capita should not, however, be interpreted as a direct measure of governance quality, management effectiveness or operational coordination. For contingency planning, the result draws attention to the wider operating environment in which port recovery takes place. Coordination with local authorities, inland transport providers and cargo stakeholders may be relevant to managing returning traffic, but the contribution of these arrangements cannot be established from the present analysis.

The findings for congestion duration and cumulative congestion impact are less conclusive. Under the selected LASSO specification, none of the candidate predictors was retained for CRD or CCI. This does not imply that static port characteristics are unimportant, nor does it establish that dynamic operational decisions are the principal determinants of congestion clearance. Rather, the examined predictors did not provide a selected explanatory relationship for these outcomes under the adopted model settings. From an operational perspective, monitoring the developing queue, returning vessel demand and available service resources may nevertheless help inform decisions on vessel admission, pilotage coordination and berth allocation. CRD and CCI provide complementary outcome measures for assessing the duration and cumulative consequences of congestion, although the effectiveness of management interventions remains to be evaluated.

For shipping companies, the distinction between congestion severity and clearance duration has implications for voyage planning and schedule recovery. A port experiencing a relatively limited congestion peak may still face prolonged delays, while a more pronounced accumulation of vessels may be cleared over a shorter period. Where suitable information is available, arrival planning and port selection can therefore consider both the extent of vessel accumulation and the progress of congestion clearance. Updated information on port operating conditions may also support adjustments to vessel arrival schedules during the recovery period.

Finally, the analysis provides a basis for considering port responses within a wider regional context. The case-identification procedure initially considered ports in the region affected by each tropical cyclone, subject to subsequent activity-based screening. This allows differences in the responses of multiple ports associated with the same cyclone event to be examined. Nevertheless, the port-cyclone case remains the unit of analysis, and the present models do not explicitly estimate inter-port substitution, traffic diversion or cascading disruption. Vessel rerouting, simultaneous disruption of neighbouring ports and coordinated reopening may influence the distribution and timing of returning traffic, but these mechanisms were not directly tested. Future research could incorporate inter-port vessel movements and regional network dependencies to examine how disruption and recovery at one port affect

congestion at others. Such analysis would extend the present port-level framework towards a network-based assessment of maritime transport resilience.

6. Conclusions

This study developed an AIS-based two-phase framework to assess port resilience by distinguishing direct disruption from subsequent post-cyclone congestion. The framework uses the PSP indicator and seven resilience indices to quantify the magnitude, duration and cumulative impact of the two phases. Unlike assessments that focus primarily on the initial disruption and return towards baseline activity, the proposed approach also captures congestion-related deviations that may occur during the subsequent recovery period. The framework accommodates heterogeneous operational responses, with the W-shaped PSP pattern serving as a conditional diagnostic representation rather than an independently established or universal resilience trajectory.

Of the 76 cyclone-port cases examined, 56 (73.7%) were classified as exhibiting direct disruption followed by post-cyclone congestion under the reference identification settings. Within the common sample used to calculate the resilience indices, the mean congestion recovery duration (CRD, 147 h) exceeded the mean direct-disruption recovery duration (TRD, 59 h), while the mean cumulative congestion impact (CCI, 77.8) was greater than the corresponding direct-disruption impact (TCI, 46.9). The LME analysis further identified an association between the congestion state and longer vessel waiting times, whereas no statistically significant association with berthing time was detected. Together, these findings demonstrate the value of considering post-cyclone congestion as a distinct component of port operational resilience, without treating the observed response sequence as independent validation of a W-shaped recovery curve.

The regression analysis identified different associations across the resilience outcomes. Container traffic share was associated with shorter direct and overall recovery durations, while facility capacity and port-city GDP per capita were positively associated with congestion residual capacity. Recorded cyclone exposure frequency was negatively associated with cumulative direct-disruption impact. No candidate predictors were retained for congestion duration or cumulative congestion impact under the selected LASSO specification. These findings indicate that the examined port characteristics and contextual variables are associated with some dimensions of recovery but do not provide a consistent explanation across all resilience outcomes. The results should therefore be interpreted as observational associations.

The study is limited to AIS-derived vessel activity and does not directly capture terminal operations, yard capacity or landside logistics. The analysis also does not explicitly account for event-specific cyclone intensity, local exposure, operational restrictions or inter-port dependencies, all of which may contribute to differences in observed recovery patterns. Future research should integrate more detailed operational and network-level data to examine the mechanisms underlying congestion development and clearance, assess the effects of recovery interventions, and evaluate the framework across other disruption contexts. Such extensions would help establish the wider applicability of the two-phase approach to maritime transport and other infrastructure systems.

CRediT authorship contribution statement

Ruikai Sun: Writing – original draft, Validation, Software, Methodology, Formal analysis, Data curation, Conceptualization, Visualization, Writing – review & editing. **Huanhuan Li:** Writing – review & editing, Visualization, Supervision, Investigation, Project administration, Validation. **Zaili Yang:** Writing – review & editing, Supervision, Funding acquisition, Conceptualization, Methodology, Resources.

Declaration of competing interest

The authors declare that they have no known competing financial interests or personal relationships that could have appeared to influence the work reported in this paper.

Acknowledgment

This project has received funding from the European Research Council (ERC) under the European Union's Horizon 2020 research and innovation programme (Grant Agreement No. 864724).

Appendix

Table A.1 reports the response type counts obtained when each identification parameter was varied individually.

Table A1
Sensitivity test of the response type classification.

Parameters	Test value	Type I	Type II	Type III	Type IV
Reference	-	56	10	8	2
Normal band	±15%	56	12	5	3
	±25%	52	12	10	2
Moving average window	12 h	55	10	9	2
	16 h	55	11	8	2
	20 h	55	10	9	2
	28 h	54	10	9	3
	32 h	55	10	8	3
	36 h	53	11	9	3
Final stable recovery	12 h	56	8	9	3
	24 h	56	9	8	3
	36 h	56	9	8	3
Congestion association	5 days	54	13	8	1
	6 days	55	11	8	2
	8 days	56	10	8	2

Note: The reference specification uses a ± 20% normal operating band, a 24-hour moving average window, a 48-hour final stable-recovery requirement and a 7-day congestion association window.

Data availability

The authors do not have permission to share data.

References

[1] Liang M, Cai Y, Chen T, Wang H, Meng Q. Data-driven impact analysis of chokepoint on multi-scale maritime networks: a case study of the Taiwan Strait. Transp Res Part E Logist Transp Rev 2025;200:104179.
[2] Sun R, Abouarghoub W, Demir E, Potter A. Geopolitical disruptions and maritime transitions: environmental and economic costs of rerouting. Transp Res Part A Policy Pract 2026;203:104737.
[3] Needham HF, Keim BD, Sathiaraj D. A review of tropical cyclone-generated storm surges: global data sources, observations, and impacts. Rev Geophys 2015;53(2):545–91.
[4] Wahiduzzaman M, Cheung KK, Luo J-J, Bhaskaran PK. A spatial model for predicting North Indian Ocean tropical cyclone intensity: role of sea surface temperature and tropical cyclone heat potential. Weather Clim Extrem 2022;36:100431.
[5] Verschuur J, Koks EE, Hall JW. Port disruptions due to natural disasters: insights into port and logistics resilience. Transp Res Part D Transp Environ 2020;85:102393.
[6] Cao X, Lam JSL. Simulation-based catastrophe-induced port loss estimation. Reliab Eng Syst Saf 2018;175:1–12.
[7] Jian W, Liu C, Lam JSL. Cyclone risk model and assessment for East Asian container ports. Ocean Coast Manag 2019;178:104796.
[8] Poo MC-P, Yang Z, Dimitriu D, Qu Z, Jin Z, Feng X. Climate change risk indicators (CCRI) for seaports in the United Kingdom. Ocean Coast Manag 2021;205:105580.
[9] Zhang C, Zhao P, Huang Z, He Z, Niu Y, Huang G, Chen Y. Assessing vessel transportation delays affected by tropical cyclones using AIS data and a Bayesian network: a case study of veronica in northwestern Australia. Ocean Eng 2024;308:118385.
[10] Li C, Yang X, Yang D. Port vulnerability to natural disasters: an integrated view from hinterland to seaside. Transp Res Part D Transp Environ 2025;139:104563.
[11] Shafieezadeh A, Ivey Burden L. Scenario-based resilience assessment framework for critical infrastructure systems: case study for seismic resilience of seaports. Reliab Eng Syst Saf 2014;132:207–19.
[12] Zhang Y, Lam JSL. Estimating the economic losses of port disruption due to extreme wind events. Ocean Coast Manag 2015;116:300–10.
[13] Wang T, Ng AKY, Wang J, Chen Q, Pang J, Tang J. Adaptation planning of container ports in the context of typhoon risks: the case of Ningbo-Zhoushan port in China. Ocean Coast Manag 2024;257:107303.
[14] Huang Z, He Z, Zhao P, Zhang C, Niu Y, Guo W, Cui Y, Shao W. The effects of tropical cyclone on the container shipping network: a case study of typhoon Ma-on (2022). Transp Res Part D Transp Environ 2024;136:104449.
[15] Mou N, Xu H, Liu Y, Li G, Zhang L, Ducruet C, Zhang X, Wang Y, Yang T. Does the Chinese coastal ports disruption affect the reliability of the maritime network? Evidence from port importance and typhoon risk. Int J Appl Earth Observ Geoinf 2024;129:103846.
[16] Shen Z, Xu X, Li J, Wang S. Vulnerability of the maritime network to tropical cyclones in the Northwest Pacific and the Northern Indian Ocean. Sustainability 2019;11(21):6176.
[17] Touzinsky KF, Scully BM, Mitchell KN, Kress MM. Using empirical data to quantify port resilience: hurricane Matthew and the Southeastern seaboard. J Waterw Port Coast Ocean Eng 2018;144(4):05018003. https://doi.org/10.1061/(ASCE)WW.1943-5460.0000446.
[18] Henry D, Emmanuel Ramirez-Marquez J. Generic metrics and quantitative approaches for system resilience as a function of time. Reliab Eng Syst Saf 2012;99:114–22.
[19] Poulin C, Kane MB. Infrastructure resilience curves: performance measures and summary metrics. Reliab Eng Syst Saf 2021;216:107926.
[20] Tang M, Zhang Y, Li C, Song Y, Huang H, Niu W, Zhang C. Assessment of port resilience based on evidential reasoning and Bayesian network: an improved framework by segmenting the metrics across time and performance dimensions. Reliab Eng Syst Saf 2025;262:111172. https://doi.org/10.1016/j.ress.2025.111172.
[21] Tsoulfas GT. Port resilience: a systematic literature review. Marit Econ Logist 2026;28:388–408.
[22] Wan C, Yang Z, Zhang D, Yan X, Fan S. Resilience in transportation systems: a systematic review and future directions. Transp Rev 2018;38(4):479–98.
[23] León-Mateos F, Sartal A, López-Manuel L, Quintás MA. Adapting our sea ports to the challenges of climate change: development and validation of a Port Resilience Index. Mar Policy 2021;130:104573.
[24] Wang N, Wu M, Yuen KF. Assessment of port resilience using Bayesian network: a study of strategies to enhance readiness and response capacities. Reliab Eng Syst Saf 2023;237:109394.
[25] Yang Z, Lau Y, Poo MC-P, Yin J, Yang Z. Port resilience to climate change in the Greater Bay Area. Transp Res Part D Transp Environ 2025;142:104681.
[26] Asadabadi A, Miller-Hooks E. Maritime port network resiliency and reliability through co-opetition. Transp Res Part E Logist Transp Rev 2020;137:101916.
[27] Cao Y, Xin X, Jarumaneeroj P, Li H, Feng Y, Wang J, Wang X, Pyne R, Yang Z. Data-driven resilience analysis of the global container shipping network against two cascading failures. Transp Res Part E Logist Transp Rev 2025;193:103857.
[28] Liu Q, Yang Y, Ng AKY, Jiang C. An analysis on the resilience of the European port network. Transp Res Part A Policy Pract 2023;175:103778.
[29] Gu B, Liu J, Ye X, Gong Y, Chen J. Data-driven approach for port resilience evaluation. Transp Res Part E Logist Transp Rev 2024;186:103570.
[30] Gu B, Chen J, Haralambides H, Liu J. A novel method of assessing port resilience and its positive ramifications. Marit Policy Manag 2025;52(4):642–65.
[31] Cassottana B, Shen L, Tang LC. Modeling the recovery process: a key dimension of resilience. Reliab Eng Syst Saf 2019;190:106528. https://doi.org/10.1016/j.ress.2019.106528.
[32] Little JDC. A proof for the queuing formula: l = λw. Oper Res 1961;9(3):383–7. https://doi.org/10.1287/opre.9.3.383.
[33] de la Peña-Zarzuelo I, Freire-Seoane MJ, López-Bermúdez B. New queuing theory applied to port terminals and proposal for practical application in container and bulk terminals. J Waterw Port Coast Ocean Eng 2020;146(1):04019031. https://doi.org/10.1061/(ASCE)WW.1943-5460.0000535.
[34] Easa SM. Approximate queueing models for analyzing harbor terminal operations. Transp Res Part B Methodol 1987;21(4):269–86. https://doi.org/10.1016/0191-2615(87)90027-0.
[35] Kiani M, Bonsall S, Wang J, Wall A. A break-even model for evaluating the cost of container ships waiting times and berth unproductive times in automated quayside operations. WMU J Marit Aff 2006;5(2):153–79. https://doi.org/10.1007/BF03195102.
[36] Saeed N, Larsen OI. Application of queuing methodology to analyze congestion: a case study of the Manila International Container Terminal, Philippines. Case Stud Transp Policy 2016;4(2):143–9. https://doi.org/10.1016/j.cstp.2016.02.001.
[37] Guo S, Wang H, Wang S. Network disruptions and ripple effects: queueing model, simulation, and data analysis of port congestion. J Mar Sci Eng 2023;11(9):1745. https://doi.org/10.3390/jmse11091745.
[38] Mohsendokht M, Kontovas C, Chang C-H, Qu Z, Li H, Yang Z. Resilience analysis of seaports: a critical review of development and research directions. Marit Policy Manag 2024;0(0):1–36.
[39] Rodrigue, J.-P., & Wildgoose, N. (2022). *Building capacity to manage risks and enhance resilience: a guidebook for ports*.
[40] Chen H, Cullinane K, Liu N. Developing a model for measuring the resilience of a port-hinterland container transportation network. Transp Res Part E Logist Transp Rev 2017;97:282–301.
[41] Zhang Y, Wei K, Shen Z, Bai X, Lu X, Soares CG. Economic impact of typhoon-induced wind disasters on port operations: a case study of ports in China. Int J Disaster Risk Reduct 2020;50:101719.
[42] Peugh JL. A practical guide to multilevel modeling. J Sch Psychol 2010;48(1):85–112.
[43] Chen W, Chen J, Geng J, Ye J, Yan T, Shi J, Xu J. Monitoring and evaluation of ship operation congestion status at container ports based on AIS data. Ocean Coast Manag 2023;245:106836.
[44] Ma J, Zhou Y, Zhu Z. Identification and analysis of ship waiting behavior outside the port based on AIS data. Sci Rep 2023;13(1):11267.
[45] IMF PortWatch. Global disaster alert and coordination system (GDACS. University of Oxford; 2025 [Data set], https://portwatch.imf.org/.
[46] LSEG. (2025). *Shipping data* [Data set]. https://www.lseg.com/en.
[47] Chen S, Meng Q, Jia P, Kuang H. An operational-mode-based method for estimating ship emissions in port waters. Transp Res Part D Transp Environ 2021;101:103080.
[48] IMO. Fourth IMO greenhouse gas study 2020. International Maritime Organization; 2020. https://greenvoyage2050.imo.org/wp-content/uploads/2021/07/Fourth-IMO-GHG-Study-2020-Full-report-and-annexes_compressed.pdf.
[49] Sun R, Abouarghoub W, Demir E. Enhancing data quality in maritime transportation: a practical method for imputing missing ship static data. Ocean Eng 2025;315:119722.
[50] Johnson H, Styhre L. Increased energy efficiency in short sea shipping through decreased time in port. Transp Res Part A Policy Pract 2015;71:167–78.